

uv Photoemission for Rare Gases Implanted in Ge

B. J. Wacławski and J. W. Gadzuk

National Bureau of Standards, Washington, D. C. 20234

and

J. F. Herbst

Physics Department, General Motors Research Laboratories, Warren, Michigan 48090

(Received 15 March 1978)

The first ultraviolet photoemission spectra of the valence electrons of rare-gas atoms, implanted by ion bombardment into an amorphous Ge matrix, are presented here. The positions of the peaks in the observed spectra are shifted relative to gas-phase spectra, consistent with a final-state screening-energy shift which varies inversely with the radius of the particular implant, as predicted by a linear-response relaxation model described herein.

If photoelectron spectroscopy of the solid state is to fulfill its promise of providing detailed information concerning the chemical environment around constituent atoms, the origin and nature of the shifts in electron binding energies of free atoms as they are incorporated into a solid must be understood.¹ We report herein the first measurements of uv photoelectron spectra ($h\nu = 21.2$ eV) for Xe, Kr, Ar, and Ne implanted by ion bombardment in Ge. We chose these systems because the chemical bonding interactions between these neutral implants and the host are small. Thus the changes between the gas and implant spectra arise mainly from initial-state electrostatic shifts, final-state extra-atomic relaxation or screening shifts, and solid-state broadening.¹ From a comparison with the gas-phase spectra, and using a linear-response theory, it is shown that the major variation in valence-level shifts can be qualitatively understood as resulting from the change in screening energy with the size of the implant atom.

The uv photoemission apparatus has been described elsewhere.² However, for the present study an ion-sputter gun and a low-energy-electron-diffraction (LEED)/Auger electron gun were added for use in sample preparation. Usual ultra-high vacuum techniques were used to obtain a base pressure of $\sim 10^{-8}$ Pa ($\sim 10^{-10}$ Torr) or less. An almost intrinsic, 50- Ω cm Ge(111) crystal, 7.5 mm square \times 1 mm thick, was mounted in a sheet molybdenum holder. The sample was annealed by resistive heating of the Mo holder. Post-bake-out cleaning of the Ge sample consisted of alternate sputtering and annealing cycles amounting to a total of about 9 h of argon-ion bombardment (5.5 μ A at 1 keV) and about 1 h of annealing at < 1000 K.³ Rare-gas ions of 1 keV were implanted with a typical dose of $\sim 10^{16}$ ions/cm², which was

found to be sufficient to saturate the UPS spectrum of the implant. During the implantation procedure, the Ge was amorphized (at least within the depth probed at $h\nu = 21.2$ eV) as evidenced by the lack of any remaining Ge(111) structure in the UPS spectra.

The spectra obtained for the series of rare gases are compared in Fig. 1, where the electron energy distributions are plotted against energy below the Fermi energy. The rare gases were implanted and spectra measured at room temperature. A measurement of the spectrum from the Mo sample holder was used to locate the Ge Fermi level. The lowest curve in the figure shows the complete spectrum for Xe in Ge, where-

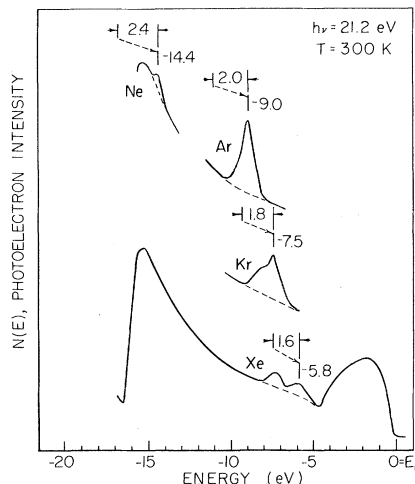


FIG. 1. Photoelectron energy distributions for rare-gas implants in amorphous Ge. Vertical lines closest to the spectra indicate measured positions of outer-shell $p_{3/2}$ levels for each implant. The upward shifts relative to the corresponding gas-phase levels are also indicated.

as, for clarity, only the ~ 5 -eV range about the structure for the other implants is shown. Dashed lines below the structure delineate the Ge background. Compared to the gas phase,⁴ the UPS spectra for the implant structure is considerably broadened. Only for Xe are the two spin-orbit-split states well resolved. A shoulder on the high-binding-energy side of the Kr spectrum corresponds to the $4p_{3/2}$ level, while the spin-orbit-split states are not resolved in the Ar and Ne spectra. It is estimated that, in addition to the spin-orbit splitting and the instrumental resolution (~ 0.2 eV), there is an additional broadening (full width at half-maximum) for the implants ranging from ~ 0.8 eV for Xe, to ~ 0.3 eV for Ne, which will be discussed in a forthcoming work.

The vertical lines closest to the photoemission spectra show the measured peak positions corresponding to the outer-shell $p_{3/2}$ electrons of each implant. Dashed lines connect these to the positions of the corresponding gas-phase ionization potentials.^{4,5} The differences between the gas-phase and implant levels are the binding-energy shifts designated by ΔE_B^0 in Table I. ΔE_B^0 is found to decrease monotonically with the progression Ne \rightarrow Xe and in fact varies inversely with R , the implant radius. Furthermore, since the size of an atom is a function of its atomic number Z , this can also be viewed as stating that ΔE_B^0 depends essentially on the atomic number of the implant, as Lang and Williams have noted in their study of chemisorbed systems.⁶

A number of different theoretical methods for estimating extra-atomic screening-energy shifts in solids have been developed during the past decade.⁶⁻¹⁰ Because of both the physical transparency and ease of utilization, we here estimate the screening-energy contribution to the valence-level shifts by employing a linear-dielectric-response theory.^{9,10} The validity of a linear response, for present applications, has been established by Williams and Lang.^{6b} The screening

energy, given as the Coulomb attraction between the hole and induced charge distributions, $\rho_0(\vec{r})$ and $\rho_{in}(\vec{r})$, respectively, is

$$\Delta_s = \frac{1}{2} \int d^3r d^3r' \rho_{in}(\vec{r}') \frac{e^2}{|\vec{r} - \vec{r}'|} \rho_0(\vec{r}). \quad (1)$$

In linear response, the Fourier components of the induced and hole charge are related as $\rho_{in}(\vec{q}) = [\{\epsilon_{ts}(q, 0) - 1\} / \epsilon_{ts}(q, 0)] \rho_0(\vec{q})$, with $\epsilon_{ts}(q, 0)$ the *total system* dielectric function, to be discussed shortly. For a spherically symmetric hole charge distribution, which is the case for the systems considered here, Eq. (1) can be Fourier transformed to [see Eq. (13) of Ref. 10]

$$\Delta_s = \frac{e^2}{\pi} \int_0^\infty dq \left[\frac{\epsilon_{ts}(q, 0) - 1}{\epsilon_{ts}(q, 0)} \right] |\rho_0(q)|^2. \quad (2)$$

To go further, the correct dielectric function, or some approximation to it, is needed.

Lang and Williams⁶ have recently found, through detailed density-functional calculations of core hole screening of atoms adsorbed on jellium surfaces, that the screening energies and induced charge are often determined by the properties of the lowest unfilled atomic orbital of the adsorbate (or in our case, the implant) and not by those of the host. The physical origin of this effect, as appropriate to closed-shell systems of the type considered in this paper, is the fact that the screening electrons must be in states that are orthogonal to the occupied core and valence states of the adsorbate (or implant). Hence, the screening charge is located outside the valence shell (although this is far from the case for open-shell atoms such as transition metals).^{6a} Ideally, this information would be built into our theory through the response function of the *total system* (host plus implant). Short of an exact calculation for each coupled system, some meaningful procedure for utilization of the (presumably known) pure host dielectric function is required. Note that the orthogonalization (to implant states) proce-

TABLE I. Comparison of various calculated and experimental binding-energy shifts for rare-gas implants in Ge (energies in eV and radii in Å).

Implant	ΔE_B^0 (expt)	R_{gas}	R_{met}	Δ_s^{gas}	Δ_s^{met}	$\Delta_s^{\text{CH}^a}$
Ne	2.4	1.58	1.83	3.98	3.50	4.35
Ar	2.0	1.88	2.26	3.41	2.88	3.85
Kr	1.8	2.00	2.42	3.22	2.70	3.4
Xe	1.6	2.17	2.62	2.99	2.51	3.25

^aSee Citrin and Hamann, Ref. 1.

ture mostly alters the short-wavelength or large- q portion of the host response function (large is $\approx 1/R_c$ where R_c is some characteristic radius for the screening charge). In effect, the orthogonalization greatly reduces the large- q response since this corresponds to the real-space region, within the geometrical domain of the implant, from which the screening electrons have been excluded. The numerical results of Lang and Williams⁶ relevant to this study, if submitted to Fourier decomposition, would consist mainly of components with $q \lesssim 1/R_c$. In this region, the system dielectric function is expected to be similar to that of the pure host. A reasonable approximation which handles the effects just discussed is to replace the total system dielectric function $\epsilon_{ts}(q, 0)$ by that of the host, $\epsilon_H(q, 0)$, and introduce an upper cutoff on the q integral,¹¹ $q_{\max} \approx \pi/2R_c$. We are then left with a picture in which

some charge distribution $\rho_0(r)$, totally within a sphere of radius R_c , induces a charge $\rho_{in}(r)$, totally outside the sphere. From elementary electrostatics, the Coulomb energy, Eq. (1), must then be independent of the specifics of $\rho_0(r)$. The simplest is a delta function at the origin, which gives $\rho(q) = 1$. Consequently Eq. (2) reduces to

$$\Delta_s \approx \frac{e^2}{\pi} \int_0^{\pi/2R_c} dq \left[\frac{\epsilon_H(q, 0) - 1}{\epsilon_H(q, 0)} \right]. \quad (3)$$

For $\epsilon_H(q, 0)$ we use the q -dependent form of the Penn dielectric function¹² due to Inkson¹³ and Resta¹⁴:

$$\epsilon_H(q, 0) = 1 + \frac{\epsilon_0 - 1}{1 + aq^2}, \quad (4)$$

in which $\epsilon_0 = 16$, $a \equiv (\epsilon_0 - 1)/\kappa_s^2$, and $\kappa_s \approx 2 \text{ \AA}^{-1}$ for Ge.¹⁴ Using Eq. (4) in Eq. (3) and performing the integration, our final expression for the screening energy is:

$$\Delta_s = \frac{e^2 \kappa_s}{2} \left(\frac{\epsilon_0 - 1}{\epsilon_0} \right)^{1/2} \left\{ 1 - \frac{2}{\pi} \tan^{-1} \left[\frac{2\kappa_s R_c}{\pi} \left(\frac{\epsilon_0}{\epsilon_0 - 1} \right)^{1/2} \right] \right\} = \left(\frac{\epsilon_0 - 1}{\epsilon_0} \right) \frac{e^2}{2R_c} \left[1 - \frac{\epsilon_0 - 1}{12\epsilon_0} \left(\frac{\pi}{\kappa_s R_c} \right)^2 + \dots \right], \quad (5)$$

which contains the physically important functional relation between the screening energy and the implant size. To first order $\Delta_s \propto 1/R_c$. We must still assign numerical values to R_c . Among the possibilities are half the nearest-neighbor distance in the corresponding inert gas solid, or a characteristic radius for the valence electron orbital of the alkali atom one atomic number above the corresponding rare gas, as this is a measure of extent of the screening charge.

The results are presented in Table I. The first and second columns list the implant species and experimentally observed binding-energy shifts. Columns three and four give the approximations used for R_c : R_{gas} , from the inert gas solid; and R_{met} , the metallic radii for the alkalis. Screening or polarization energies calculated from Eq. (5) for a Ge host using radii in columns three and four are shown in columns five and six, respectively. The experimental shift consists of two contributions, a so-called initial-state electrostatic (chemical) shift to higher binding energy, due to D , the dipole potential barrier at the Ge surface, which is independent of the implant species,¹⁵ and the "final-state" screening shift calculated here; that is, $\Delta E_B^0(\text{expt}) \approx \Delta_s - D$. Using the calculated values for Δ_s^{gas} and Δ_s^{met} , and the observed total shift ΔE_B^0 , dipole barriers $D(\text{gas}) \approx 1.4 \pm 0.2 \text{ eV}$ or $D(\text{met}) \approx 0.9 \pm 0.15 \text{ eV}$, can be inferred for the entire set of implants. Fur-

ther, we note that for the range of plausible R_c values in Table I, the corresponding calculated values for Δ_s track the observed variation in ΔE_B^0 . Thus, the screening contribution can qualitatively account for the change in binding-energy shift with implant. The major point is that to within experimental resolution limitations, the observed shifts are consistent with an interpretation in terms of an implant-independent constant shift D due to the surface dipole plus a screening shift Δ_s which varies inversely with implant size. Although the relative contributions of D and Δ_s differ depending on choice of R_c , our interpretation of the total observed shifts are in accord with either set of values for R_c . Finally, Citrin and Hamann,¹ using a self-consistent density-functional method, calculated the core-hole polarization energies for rare-gas implants in noble-metal hosts shown in column seven. Although their values were calculated for core ionization and different hosts, the fact that Δ_s varies inversely with R is the physically significant feature, and this is contained in each of the theories.

We wish to thank Art Williams, IBM Yorktown Heights, for constructive comments.

¹P. H. Citrin and D. R. Hamann, Chem. Phys. Lett.

22, 301 (1973), and Phys. Rev. B **10**, 4948 (1974); K. S. Kim and N. Winograd, Chem. Phys. Lett. **30**, 91 (1975); R. E. Watson, J. F. Herbst, and J. W. Wilkins, Phys. Rev. B **14**, 18 (1976); D. A. Shirley, R. L. Martin, S. P. Kowalczyk, F. R. McFeely, and L. Ley, Phys. Rev. B **15**, 544 (1977).

²E. W. Plummer, B. J. Wacławski, T. V. Vorburger, and C. E. Kuyatt, Prog. Surf. Sci. **7**, 149 (1976).

³A W-(W/Re) thermocouple was spot welded to the rear of the crystal holder, so that the temperature of the Ge was not measured directly. Therefore, only the possible maximum temperature of the Ge crystal can be given with any certainty.

⁴D. W. Turner, A. D. Baker, C. Baker, and C. R. Brundle, *Molecular Photoelectron Spectroscopy* (Wiley-Interscience, New York, 1970).

⁵In order to refer the gas-phase ionization potentials to E_F , the sample work function, $\phi(\text{Ge})$, must be known. $\phi(\text{Ge})$ was found to be independent of the particular implant and was equal to 4.75 ± 0.05 eV, as determined from the difference between the photon energy and the width of the photoelectron distribution from Ge.

^{6a}N. D. Lang and A. R. Williams, Phys. Rev. B **16**, 2408 (1977).

^{6b}A. R. Williams and N. D. Lang, Phys. Rev. Lett. **40**, 954 (1978).

⁷L. Hedin and A. Johansson, J. Phys. B **2**, 1336 (1969).

⁸See *Elementary Excitations in Solids, Molecules, and Atoms*, edited by J. T. Devreese, A. B. Kunz, and T. C. Collins (Plenum, New York, 1974); *Electron and Ion Spectroscopy of Solids*, edited by L. Fiermans, R. Hoogewijs, and J. Vennik (Plenum, New York,

1978). Other surveys to check are *Electron Spectroscopy: Theory, Techniques and Applications*, edited by C. R. Brundle and A. D. Baker (Academic, London, 1977); *Photoemission and the Electronic Properties of Surfaces*, edited by B. Feuerbacher, B. Fitton, and R. Willis (Wiley, London, 1978).

⁹L. Hedin and S. Lundqvist, in *Solid State Physics*, edited by H. Ehrenreich, F. Seitz, and D. Turnbull (Academic, New York, 1969), Vol. 23, p. 1.

¹⁰J. W. Gadzuk, Phys. Rev. B **14**, 2267 (1976).

¹¹Indeed there is some arbitrariness in relating the q cutoff to a real-space parameter. Our choice is based on the following considerations. For density fluctuations whose wavelengths satisfy $\lambda/2 \leq 2R$ (or equivalently $q \geq 2/\pi R_c$) cancellations in the overlap of hole charge within the sphere of radius R_c and induced density components outside occur. In addition, this choice yields the final result of Eq. (5) in the form of the correct classical result plus modifications due to the q dependence of $\epsilon_H(q, 0)$.

¹²D. R. Penn, Phys. Rev. **128**, 2093 (1962).

¹³J. C. Inkson, J. Phys. C **5**, 2599 (1972); P. W. Anderson, in *Elementary Excitations in Solids, Molecules, and Atoms*, edited by J. T. Devreese, A. B. Kunz, and T. C. Collins (Plenum, New York, 1974).

¹⁴R. Resta, Phys. Rev. B **16**, 2717 (1977).

¹⁵Another "chemical shift" could result from a possible implant-dependent difference in electrostatic potential between the implant site and the average internal potential within the Ge. With the spirit of simple linear-response theory, this shift can either be neglected or be incorporated into the surface dipole form, as discussed in great detail in Ref. 1.

Macroscopic Effect of P - and T -Nonconserving Interactions in Ferroelectrics: A Possible Experiment?

A. J. Leggett

School of Mathematical and Physical Sciences, University of Sussex, Brighton BN1 9QH, Sussex, United Kingdom,^(a) and Physics Department, University of Science and Technology, Kumasi, Ghana

(Received 20 April 1978)

In the presence of interactions which violate both P and T invariance, a ferroelectric crystal with electric polarization \vec{P} and appreciable nuclear spin polarization, suspended in a magnetic field \vec{H} , will experience a torque of the form $\vec{P} \times \vec{H}$. The maximum torque density in PbTiO_3 compatible with existing limits on such interactions is estimated at a few times 10^{-6} erg/cm³. Some obvious "nuisance" effects are estimated and the theoretical sensitivity of such an experiment discussed.

In view of the current poor understanding of the mechanism of CP nonconservation in the weak interaction,¹ it is of considerable interest to search for effects of the accompanying violation of time-reversal invariance (T) which is then required by the CPT theorem. The most obvious manifestation of such an effect is the existence of an elec-

tric dipole moment (EDM) directed along the total angular momentum \vec{J} of a particle, atom or molecule; this requires, of course, simultaneous non-conservation of P and T . Apart from experiments on the free neutron,² the main experiments in this area^{3,4} have searched for a linear Stark effect in atoms or molecules; originally designed to look